bioRxiv preprint doi: https://doi.org/10.1101/2021.09.01.458261; this version posted April 1, 2022. The copyright holder for this preprint (which was not certified by peer review) is the author/funder, who has granted bioRxiv a license to display the preprint in perpetuity. It is made available under aCC-BY 4.0 International license.

The *Shigella* type III effector protein OspB is a cysteine protease

Thomas E. Wood,[1,2] Kathleen A. Westervelt,[1,3] Jessica M. Yoon,[4,7] Heather D. Eshleman,[1,2,8] Roie Levy,[1,2] Henry Burnes,[5] Daniel J. Slade,[6] Cammie F. Lesser,[1,2] Marcia B. Goldberg[1,2,*]

[1]Department of Medicine, Division of Infectious Diseases, Massachusetts General Hospital, Boston, Massachusetts, USA.

[2]Department of Microbiology, Blavatnik Institute, Harvard Medical School, Boston, Massachusetts, USA.

[3]Department of Immunology and Infectious Diseases, Harvard T. H. Chan School of Public Health, Boston, Massachusetts, USA.

[4]Department of Molecular and Cellular Biology, Harvard University, Cambridge, Massachusetts, USA.

[5]Department of Chemistry and Chemical Biology, Harvard University, Cambridge, Massachusetts, USA.

[6]Department of Biochemistry, Virginia Polytechnic Institute and State University, Blacksburg, Virginia, USA

[7]Present address: Office of Response and Recovery, Federal Emergency Management Agency, Washington, D.C., USA

[8]Present address: Lexical Intelligence, LLC, Rockville, Maryland, USA

[*]For correspondence: E-mail: marcia.goldberg@mgh.harvard.edu Tel: +1 617-525-4820.

bioRxiv preprint doi: https://doi.org/10.1101/2021.09.01.458261; this version posted April 1, 2022. The copyright holder for this preprint (which was not certified by peer review) is the author/funder, who has granted bioRxiv a license to display the preprint in perpetuity. It is made available under aCC-BY 4.0 International license.

Abstract

The type III secretion system is required for virulence of many pathogenic bacteria. Bacterial effector proteins delivered into target host cells by this system modulate host signaling pathways and processes in a manner that promotes infection. Here, we define the activity of the effector protein OspB of the human pathogen *Shigella* spp., the etiological agent of shigellosis and dysenteric disease. Using the yeast *Saccharomyces cerevisiae* as a model organism, we show that OspB sensitizes cells to inhibition of TORC1, the central regulator of growth and metabolism. *In silico* analyses reveal that OspB bears structural homology to bacterial cysteine proteases, and we define a conserved cysteine-histidine catalytic dyad required for OspB function. Using yeast genetic screens, we identify a crucial role for the arginine N-degron pathway in the growth inhibition phenotype and show that inositol hexakisphosphate is an OspB cofactor. We find that a yeast substrate for OspB is the TORC1 component Tco89p, proteolytic cleavage of which generates a C-terminal fragment that is targeted for degradation *via* the arginine N-degron pathway; processing and degradation of Tco89p is required for the OspB phenotype. In all, we demonstrate that the *Shigella* T3SS effector OspB is a cysteine protease and decipher its interplay with eukaryotic cell processes.

Importance

Shigella spp. are important human pathogens and one of the leading causes of diarrheal mortality worldwide, especially in children. Virulence depends on the *Shigella* type III secretion system (T3SS), and definition of the roles of the bacterial effector proteins secreted by the T3SS is key to understanding *Shigella* pathogenesis. The effector protein OspB has been shown to contribute to a range of phenotypes during infection, yet the mechanism of action is unknown. Here, we show that OspB possesses cysteine protease activity in both yeast and mammalian cells, and that enzymatic activity of OspB depends on a conserved cysteine-histidine catalytic dyad. We determine how its protease activity sensitizes cells to TORC1 inhibition in yeast, finding that OspB cleaves a component of yeast TORC1, and that the degradation of the C-terminal cleavage product is responsible for OspB mediated hypersensitivity to

bioRxiv preprint doi: https://doi.org/10.1101/2021.09.01.458261; this version posted April 1, 2022. The copyright holder for this preprint (which was not certified by peer review) is the author/funder, who has granted bioRxiv a license to display the preprint in perpetuity. It is made available under aCC-BY 4.0 International license.

TORC1 inhibitors. Thus, OspB is a cysteine protease that depends on a conserved cysteine-histidine catalytic dyad.

Keywords

Shigella, OspB, cysteine protease, TORC1, N-degron

Introduction

Cellular processes are largely controlled by both the availability of nutrients and the ability to respond to these environmental cues. Consequently, homeostatic control of metabolism is crucial to function, growth and ultimately viability. The balance between anabolic and catabolic processes in eukaryotes is controlled by the target of rapamycin (TOR) complex, a large multi-subunit hub integrating sensory inputs to regulate cellular metabolism. In nutrient-replete conditions, amino acid and glucose availability sustains the kinase activity of the TORC1 complex, promoting translation, gene expression and protein stability. In contrast, cellular stresses and starvation inhibit TORC1-dependent growth and stimulate proteolytic mechanisms such as autophagy to maintain amino acid pools (González & Hall, 2017).

Infection perturbs cellular homeostasis (Eisenreich et al., 2013). Pathogens that invade host cells disrupt cellular processes in ways that promote the survival and replication of the infectious agent. *Shigella* spp. are the etiological agent of bacillary dysentery and a leading contributor to diarrheal mortality (Khalil et al., 2018). This pathogen invades the intestinal epithelium, establishing a replicative niche within colonic epithelial cells and triggering an acute inflammatory immune response (Carayol & Tran Van Nhieu, 2013). The type III secretion system (T3SS) is required for *S. flexneri* infection, facilitating invasion and bacterial replication through the delivery into host cells of effector proteins that subvert cellular signaling pathways. Effector proteins also promote the spread of intracellular *Shigella* between cells, whereby it disseminates throughout the intestinal epithelium (Agaisse, 2016).

bioRxiv preprint doi: https://doi.org/10.1101/2021.09.01.458261; this version posted April 1, 2022. The copyright holder for this preprint (which was not certified by peer review) is the author/funder, who has granted bioRxiv a license to display the preprint in perpetuity. It is made available under aCC-BY 4.0 International license.

Shigella T3SS effector proteins display a myriad of well-characterized enzymatic activities including phosphatase, acyltransferase, ubiquitin ligase and protease functions, as well as catalyzing other more unconventional biochemical modifications (Burnaevskiy et al., 2013; H. Li et al., 2007; Z. Li et al., 2021; Liu et al., 2018; Niebuhr et al., 2002; Rohde et al., 2007; Zhang et al., 2012). The effector OspB has been described by our group and others as manipulating mTORC1 signaling, dampening the innate immune response *via* MAP kinase and NF-κB signaling, and modulating cytokine release (Ambrosi et al., 2015; Fukazawa et al., 2008; Zurawski et al., 2009). However, the precise mode of action of this effector protein is unknown.

In this study, we determine that the *S. flexneri* T3SS effector OspB is a cysteine protease. *In silico* analysis indicated structural homology to bacterial cysteine proteases, permitting identification of putative catalytic residues. Using a yeast model to study the impact of OspB activity on a eukaryotic host, we determine host factors required for OspB-dependent hypersensitivity to TORC1 inhibition, including inositol phosphate biosynthesis, TORC1 signaling, and protein degradation pathways. We find that the OspB-dependent hypersensitivity phenotype is due to the cleavage of the TORC1 component Tco89p, in a manner that requires both the conserved catalytic dyad in OspB and the secondary messenger molecule inositol hexakisphosphate. Finally, we demonstrate that the C-terminal product of Tco89p cleavage enters the arginine N-degron pathway for destruction by the proteasome, and that its degradation is required for OspB-dependent growth inhibition of yeast.

Results

OspB exhibits structural homology to cysteine proteases

To gain insight into the potential mechanism of action of OspB, we performed *in silico* analyses of its amino acid sequence. This analysis revealed that OspB shares 27-30% sequence identity with the cysteine protease domains (CPD) of the large clostridial cytotoxins TcdA and TcdB of *Clostridioides difficile* and the multifunctional autoprocessing repeats-in-toxin (MARTX) RtxA toxins of *Vibrio cholerae* and *V. vulnificus* (**Fig. 1A**). TcdA, TcdB and RtxA are modular toxins that upon host cell endocytosis undergo autoproteolysis, which releases toxin domains that subvert cellular processes by

bioRxiv preprint doi: https://doi.org/10.1101/2021.09.01.458261; this version posted April 1, 2022. The copyright holder for this preprint (which was not certified by peer review) is the author/funder, who has granted bioRxiv a license to display the preprint in perpetuity. It is made available under aCC-BY 4.0 International license.

inducing actin depolymerization and altering GTPase signaling (Fullner & Mekalanos, 2000; Just et al., 1995). In contrast to these large cytotoxins, OspB is small (288 amino acids; 32 kD), and we found no evidence for OspB autoprocessing in cells (**Fig. S1** in the supplemental material).

The cysteine and histidine residues required for the proteolytic activity of the CPDs are conserved in OspB and the orthologous T3SS effector protein of *V. parahaemolyticus* VPA1380 (Calder et al., 2014; Egerer et al., 2007; Sheahan et al., 2007) (**Fig. 1A** and **Fig. S2A**). Indeed, the tertiary structure of OspB can be modelled on the CPDs of RtxA and TcdA with 96% and 62% confidence, respectively, with conservation of the positions of their catalytic residues with C184 and H144 of OspB (**Fig. 1B** and **Fig. S2B**). The alignment of OspB with the CPD structures suggested that OspB residues C184 and H144, may be required for OspB activity. A quantitative assay in yeast strains expressing *S. flexneri* effector proteins previously demonstrated that OspB causes growth inhibition of yeast in the presence of the cellular stressor caffeine (Slagowski et al., 2008). We utilized this assay to probe the role of the putative catalytic residues in OspB activity. Whereas expression of wild type OspB elicits a drastic growth defect in the presence of caffeine, mutation of either C184 or H144 completely abrogated toxicity (**Fig. 1C**). These data indicate that OspB inhibition of yeast growth depends on the predicted catalytic dyad of C184 and H144, bolstering our predictions for the tertiary structure of OspB as a structural homolog of the cysteine protease domains of several modular bacterial toxins.

Mutagenesis studies of TcdA showed that in addition to C700 and H655, D589 is required for autoprocessing through proton abstraction from the histidine in the active site (Pruitt et al., 2009). In RtxA, mutagenesis of the equivalent aspartic acid residue D3469 alone does not impact proteolytic activity; however concerted deletion of E3467 results in partial loss of autocleavage (Prochazkova & Satchell, 2008). In OspB an aspartic acid residue (D108) is predicted to be present at the equivalent position of $D589^{TcdA}$, adjacent to two additional aspartic acid residues D109 and D110 (**Fig. S2A** and **S2B**). These were therefore candidates for involvement in catalysis. Alanine substitution of none of these aspartic acid residues rescued yeast growth (**Fig. S2C**). In addition, a D108A/D110A double mutant had no effect on OspB activity. These results indicate that the function of OspB requires both a cysteine and a histidine residue, similar to the cysteine-histidine catalytic dyad of the CPD of RtxA.

bioRxiv preprint doi: https://doi.org/10.1101/2021.09.01.458261; this version posted April 1, 2022. The copyright holder for this preprint (which was not certified by peer review) is the author/funder, who has granted bioRxiv a license to display the preprint in perpetuity. It is made available under aCC-BY 4.0 International license.

Among the effects of caffeine on cellular processes, inhibition of TORC1 is described as an important mode of action for this compound in yeast (Reinke et al., 2006). To determine whether the effect of caffeine on the OspB phenotype is specific to TORC1, we replaced caffeine in the media with rapamycin, which unlike caffeine is a specific inhibitor of TORC1. As with caffeine, the presence of rapamycin sensitized yeast to growth inhibition by OspB in a manner that depended on residues C184 and H144 (**Fig. 1C**). These data indicate that the impact of OspB on yeast growth depends on inhibition of TORC1, consistent with our previous findings that OspB potentiates rapamycin inhibition of growth in mammalian cells (Lu et al., 2015). The presence of similar OspB-dependent phenotypes in both yeast and mammalian cells with respect to sensitization to TOR inhibition demonstrates that yeast present a reasonable model for investigating the mechanism of OspB activity.

Inositol hexakisphosphate is required for OspB activity

With the goal of identifying host factors required for OspB activity, we screened a *S. cerevisiae* deletion library for strains in which OspB was no longer able to inhibit yeast growth in the presence of caffeine (**Fig. 2A**). The OspB-mediated growth defect was diminished in the absence of 81 genes, including several whose gene products act downstream of TORC1 (**Table S4**). Deletion of these genes would be expected to uncouple TORC1 signaling from its downstream transcriptional response, thereby decreasing the sensitivity to TORC1 inhibitors. This validates the ability of the screen to identify host factors required for the OspB-mediated growth phenotype and confirms a role of TORC1 signaling therein.

The screen also identified *IPK1*, which encodes the enzyme responsible for the generation of inositol hexakisphosphate (IP_6), as required for yeast growth inhibition by OspB. Using an independent *ipk1* deletion strain, we confirmed that *IPK1* is required for OspB-mediated growth sensitivity to TORC1 inhibitors and found that reintroduction of *IPK1 in trans* restored growth inhibition (**Fig. 2B**). Of note, IP_6 is an allosteric activator of the CPDs of RtxA and TcdA, and it is required for cysteine protease activity *in vitro* (Prochazkova & Satchell, 2008; Reineke et al., 2007). *In vitro* data assessing the role of IP_6 and a more highly phosphorylated inositol pyrophosphate species (IP_7) in the autoprocessing of TcdB indicate that IP_7 is also a potent activator of TcdB cysteine protease activity (Savidge et al., 2011).

bioRxiv preprint doi: https://doi.org/10.1101/2021.09.01.458261; this version posted April 1, 2022. The copyright holder for this preprint (which was not certified by peer review) is the author/funder, who has granted bioRxiv a license to display the preprint in perpetuity. It is made available under aCC-BY 4.0 International license.

Since an *ipk1* mutant lacks IP_6 and all IP_7 and IP_8 inositol pyrophosphate species (Saiardi et al., 2002), we tested whether these inositol pyrophosphatase species were dispensable for OspB enzymatic activity by assessing growth inhibition in the absence of both yeast inositol hexakisphosphate kinases Kcs1p and Vip1p (Mulugu et al., 2007). The *kcs1*Δ*vip1*Δ mutant still displayed OspB-dependent sensitivity to TORC1 inhibitors, indicating that IP_6 is sufficient to stimulate the activity of OspB (**Fig. 2C**). Furthermore, we confirmed previous data (Calder et al., 2014) that showed that IP_6 is sufficient for enzymatic activation of the OspB ortholog VPA1380 from *Vibrio parahaemolyticus* (**Fig. 2D**), pointing to the Ipk1p-dependency of VPA1380 for yeast growth inhibition resulting specifically from the loss of IP_6 rather than inositol pyrophosphate species.

The arginine N-degron pathway is required for growth inhibition by OspB

Our deletion screen for host factors required for OspB-mediated sensitization of yeast to TORC1 inhibition also identified several components of the arginine N-degron pathway. This protein degradation pathway recognizes the neo-N-termini of polypeptides generated by cleavage or processing events and targets the polypeptides to the proteasome (Varshavsky, 2019). If the N-terminal residue of the C-terminal fragment produced upon protein cleavage is glutamine or asparagine, this destabilizes the fragment, directing its degradation *via* the arginine N-degron pathway (Gonda et al., 1989). The N-terminal Gln or Asn residue is deamidated to a Glu or Asp residue, respectively, by the N-terminal amidase Nta1p. The polypeptide is arginylated at the N-terminus by the arginine transferase Ate1p, permitting subsequent recruitment of the E3-E2 ubiquitin ligase N-recognin complex Ubr1p-Rad6p, which ubiquitinates the N-degron for degradation by the proteasome (**Fig. 3A**) (Baker & Varshavsky, 1995; Bartel et al., 1990; Dohmen et al., 1991; Richter-Ruoff et al., 1992).

Deletion of *nta1*, *ate1*, *ubr1*, or *rad6* each rescued the growth inhibition phenotype catalyzed by OspB (**Fig. 3B**). Moreover, introduction of a plasmid expressing *NTA1* from its native promoter complemented the *nta1* mutant, whereas complementation with a *nta1*(C187S) allele, encoding a catalytically inactive amidase, did not restore OspB-dependent sensitivity to TORC1 inhibition (**Fig. 3C** and **Fig. S3**). These results show that the host arginine N-degron pathway is required for growth

bioRxiv preprint doi: https://doi.org/10.1101/2021.09.01.458261; this version posted April 1, 2022. The copyright holder for this preprint (which was not certified by peer review) is the author/funder, who has granted bioRxiv a license to display the preprint in perpetuity. It is made available under aCC-BY 4.0 International license.

inhibition by OspB and suggests that the generation of an N-degron harboring an N-terminal Gln or Asn is a necessary step in this process.

A parallel screen using a yeast over-expression library (Sopko et al., 2006) to identify suppressors of OspB-mediated sensitivity to caffeine found that expression of *BRE1* from a multicopy vector rescued the OspB-dependent growth defect (**Table S5**). Bre1p is an E3 ubiquitin ligase that monoubiquitinates histone H2B to regulate chromatin structure, in conjunction with Rad6p as the E2 ubiquitin conjugating enzyme (Hwang et al., 2003; Wood et al., 2003). We hypothesized that the mechanism of rescue by Bre1 overexpression is its sequestration of Rad6p from the arginine N-degron pathway, effectively phenocopying a *rad6* mutant (**Fig. S4A**). We found that the E2 enzymatic activity of Rad6p is required for growth inhibition by OspB, since production of a catalytically inactive Rad6p (C88S) variant did not complement a *rad6* mutant, whereas the wild type *RAD6* allele did (**Fig. S4B**). In contrast, overexpression of a catalytically dead Bre1p (C663S) variant rescued the growth defect (**Fig. S4C**), indicating that the E3 ubiquitin ligase activity of Bre1p is dispensable for suppression of the OspB phenotype, consistent with the proposed mechanism of suppression being Rad6p sequestration. Expression of an additional copy of *RAD6* negated the suppression phenotype of Bre1p overexpression (**Fig. S4D**), suggesting that higher levels of Bre1p rescue growth through indirectly reducing flux through the arginine N-degron pathway. Taken together, these data demonstrate that the activity of the arginine N-degron pathway is critical for OspB to sensitize yeast to TORC1 inhibition.

VPA1380 expression is toxic to yeast even in the absence of TORC1 inhibitors, indicative of a mechanism divergent to that of OspB. In addition, the absence of *nta1* or other arginine N-degron pathway components did not perturb the growth inhibition elicited by VPA1380, suggesting that the outcome of its activity differs from that of OspB (**Fig. 3D & Fig. S5**). Furthermore, no role was found for the formyl-methionine or proline N-degron pathways (Chen et al., 2017; J.-M. Kim et al., 2018; Melnykov et al., 2019) in VPA1380-mediated growth inhibition (**Fig. S5**). Thus, despite the homology between OspB and VPA1380, and that both T3SS effectors inhibit yeast growth, these data suggest that these bacterial proteins elicit toxicity *via* divergent mechanisms.

bioRxiv preprint doi: https://doi.org/10.1101/2021.09.01.458261; this version posted April 1, 2022. The copyright holder for this preprint (which was not certified by peer review) is the author/funder, who has granted bioRxiv a license to display the preprint in perpetuity. It is made available under aCC-BY 4.0 International license.

OspB cleaves the TORC1 component Tco89p

Since yeast expressing OspB are sensitive to TORC1 inhibitors, we postulated that OspB either perturbs TORC1 signaling upstream of TORC1 or directly manipulates the TORC1 complex itself. Genetic ablation of individual nutrient sensing pathways upstream of TORC1 (**Fig. 4A**) (Binda et al., 2009; Dubouloz et al., 2005; Hughes Hallett et al., 2014; A. Kim & Cunningham, 2015; Yuan et al., 2017) did not rescue the OspB phenotype (**Fig. S6A**). With respect to *pib2*, which encodes a glutamine sensor that activates TORC1 in parallel to the amino acid-responsive Gtr1p/Gtr2p pathway (Tanigawa et al., 2021; Ukai et al., 2018), a yeast strain constitutively producing OspB in the absence of *pib2* could not be generated; however, expression of *ospB* from a galactose inducible promoter completely inhibited the growth of a *pib2* mutant without the need for low levels of caffeine or rapamycin (**Fig. 4B**). Genetic ablation of components of TORC1 or the Gtr1p/Gtr2p branch of amino acid sensing is synthetically lethal in a *pib2*Δ background (A. Kim & Cunningham, 2015), and we find that OspB is still toxic in a *gtr1*Δ*gtr2*Δ double mutant (**Fig. S6B**). We therefore conclude that OspB likely targets the TORC1 complex itself.

We tested whether any of the four proteins that comprise the TORC1 complex - Kog1p, Lst8p, Tco89p and Tor1p/Tor2p (Reinke et al., 2004) – are perturbed by OspB activity. Among these four proteins, only Tor1p and Tco89p are non-essential. We found that neither the essential TORC1 components nor Tor1p is cleaved by OspB (**Fig. S7A**). Since deletion of *tco89* rendered yeast hypersensitive to rapamycin (Reinke et al., 2004), it was not possible to test for an effect of OspB in this growth assay. OspB-dependent sensitivity to TORC1 inhibitors was restored upon *TCO89* complementation (**Fig. 4C)**.

Assessment of Tco89p abundance revealed that in the presence of OspB, full length Tco89p levels were decreased and a faster migrating Tco89p band that was recognized by an antibody to the C-terminal tag was present (**Fig. 4D**). This faster migrating band was not observed in the presence of the catalytically inactive OspB C184S mutant, indicating that its generation depends on OspB catalytic activity and that the faster migrating band is a C-terminal Tco89p cleavage product. Overexpression of *TCO89* in wild

bioRxiv preprint doi: https://doi.org/10.1101/2021.09.01.458261; this version posted April 1, 2022. The copyright holder for this preprint (which was not certified by peer review) is the author/funder, who has granted bioRxiv a license to display the preprint in perpetuity. It is made available under aCC-BY 4.0 International license.

type yeast rescued the OspB-dependent growth defect (**Fig. 4E**), presumably because resulting increase in Tco89p levels likely raises the threshold at which sensitivity to TORC1 inhibitors occurs.

Cleavage of endogenous Tco89p was abolished in an *ipk1* background and restored by complementation of *IPK1*, indicating that requirements for the yeast growth phenotype are associated with the Tco89p cleavage phenotype (**Fig. 4F**). Tco89p cleavage by OspB was unaffected in a *kcs1*Δ*vip1*Δ mutant (**Fig. S7B**), providing additional evidence that IP_6 is the inositol phosphate species acting as the cofactor for OspB protease activity. Transfection of mammalian cells with both OspB and Tco89p revealed that OspB cleavage of Tco89p occurs (**Fig. 4G**), which indicates that OspB functions as a protease in mammalian cells and suggests that Tco89p may be a direct substrate of OspB protease activity.

Processing of Tco89p by VPA1380 was not observed (**Fig. S8**), further supporting that the mechanisms of OspB and VPA1380 are divergent. Together, these data demonstrate that, upon its allosteric activation by IP_6, OspB cleaves the TORC1 component Tco89p triggering sensitivity to inhibition of TORC1 signaling.

We assessed the role of the arginine N-degron pathway in the stability of the C-terminal Tco89p cleavage product generated by OspB. Treatment of yeast with the proteasome inhibitor MG-132 increased the abundance of the Tco89p C-terminal fragment, indicating that this fragment is a substrate of the proteasome (**Fig. 5A**). Deletion of *nta1* resulted in an increase in the abundance of the Tco89p C-terminal fragment (**Fig. 5B**), and its levels were restored by reintroduction of *NTA1*, but not by reintroduction of the C187S inactive amidase mutant, indicating that the C-terminal fragment of Tco89p is the N-degron that mediates growth inhibition caused by the protease activity of OspB.

In summary, we found that the *Shigella* T3SS effector OspB is a cysteine protease that cleaves the TORC1 component Tco89p, thereby generating an N-degron, and that the N-degron is targeted for degradation by the arginine N-degron pathway (**Fig. 5C**). Cleavage of Tco89p by OspB and host-mediated degradation of the C-terminal fragment is responsible for sensitization of the TORC1 complex to inhibition and the associated inhibition of yeast growth.

bioRxiv preprint doi: https://doi.org/10.1101/2021.09.01.458261; this version posted April 1, 2022. The copyright holder for this preprint (which was not certified by peer review) is the author/funder, who has granted bioRxiv a license to display the preprint in perpetuity. It is made available under aCC-BY 4.0 International license.

Discussion

The evidence presented here collectively demonstrates that the *Shigella* T3SS effector OspB is a cysteine protease and that it requires inositol hexakisphosphate for its activity. OspB is required for cleavage of Tco89p, a component of yeast TORC1, and upon expression of the two proteins in mammalian cells, OspB is sufficient to cleave Tco89p (**Fig. 4**), indicating that OspB mediated cleavage of Tco89p is either direct or depends on factors that are conserved between yeast and mammalian cells. OspB is structurally homologous to the cysteine protease domains of the bacterial MARTX toxins TcdA, TcdB and RtxA, with conservation of the catalytic cysteine and histidine residues (**Fig. 1 and S2**) (Egerer et al., 2007; Lupardus et al., 2008; Reineke et al., 2007; Shen et al., 2009). In OspB, the conserved cysteine and histidine are each required for both the OspB growth inhibition phenotype in yeast and Tco89p cleavage in yeast and mammalian cells (**Fig. 4** and data not shown).

Like TcdA, TcdB and RtxA, OspB requires inositol hexakisphosphate for its activity (**Fig. 2** and **4**) (Egerer & Satchell, 2010). Using a genetic approach, we exclude inositol pyrophosphate species as being necessary for OspB activity and define the inositol phosphate species requirement as IP_6; however, it is possible that an inositol pyrophosphate species may be sufficient for stimulating activity *in vitro*, as found for IP_7 and *C. difficile* TcdB (Savidge et al., 2011). The requirement for a host-specific cofactor, such as IP_6, ubiquitin, calmodulin, or cyclophilins, for the activation bacterial effectors is increasingly appreciated (Anderson et al., 2011; Coaker et al., 2005; Drum et al., 2002; Mittal et al., 2010; Sreelatha et al., 2020; Tyson & Hauser, 2013) and necessarily restricts enzymatic activity to the context of host infection. Together, these findings provide strong evidence that OspB is a cysteine protease in the family of proteases represented by the cysteine protease domains of the MARTX toxins and large clostridial cytotoxins.

Two other *Shigella* T3SS effectors, IpaJ and OspD3, are also cysteine proteases. IpaJ and OspD3 are divergent from OspB and their substrates are distinct, constituting Rho GTPases and necroptotic signaling factors, respectively (Ashida et al., 2020; Burnaevskiy et al., 2015). Genes encoding T3SS effector proteins are often acquired by horizontal gene transfer (Brown & Finlay, 2011), thus homologous effectors are commonly secreted by the T3SSs of pathogens displaying similar host

bioRxiv preprint doi: https://doi.org/10.1101/2021.09.01.458261; this version posted April 1, 2022. The copyright holder for this preprint (which was not certified by peer review) is the author/funder, who has granted bioRxiv a license to display the preprint in perpetuity. It is made available under aCC-BY 4.0 International license.

283 tropism. The T3SS2 effector of *V. parahaemolyticus* VPA1380 is homologous to OspB, yet we find
284 that it likely targets a different host substrate. First, yeast growth inhibition by OspB requires reduction
285 of TORC1 activity by either chemical or genetic intervention (**Fig. 1** and **4**), whereas VPA1380 is toxic
286 to yeast in the absence of additional stressors (**Fig. 2**) (Calder et al., 2014). Second, we find that
287 VPA1380 neither cleaves Tco89p nor generates a substrate cleavage product that requires the arginine
288 N-degron pathway for its degradation (**Fig. 3**, **S5**, and **S8**).

289 OspB cleaves a component of TORC1 to produce a C-terminal fragment that enters the arginine N-
290 degron pathway for proteasomal degradation, rendering the cells hypersensitive to TOR inhibition.
291 Tco89p cleavage and degradation appears to be entirely responsible for the TOR inhibitor
292 hypersensitivity phenotype stimulated by OspB, as degradation of the C-terminal fragment phenocopies
293 a *tco89*Δ mutant growth defect in the presence of either rapamycin or caffeine (**Fig. 4C**) (Reinke et al.,
294 2004, 2006; Slagowski et al., 2008). Consequently, complementation with multi-copy Tco89p is
295 associated with reduced sensitivity to inhibition of TORC1 by a combination of OspB and chemical
296 inhibitors (**Fig. 4E**). The dependence on *NTA1*, the upstream-most enzyme in the arginine N-degron
297 pathway (**Fig. 3**), indicates that OspB cleavage results in a tertiary arginine N-degron, with glutamine
298 or asparagine at the neo-N-terminus of the C-terminal Tco89p cleavage product, since deamidation of
299 the product by Nta1p is a critical step in its degradation (Gonda et al., 1989).

300 The migration of Tco89p constructs in SDS-PAGE is slower (at around 150 kD) than expected for the
301 89 kD protein (**Fig. 4**). We hypothesize that the retarded migration of Tco89p is due to significant
302 phosphorylation by the TORC1 kinase (Huber et al., 2009; Oliveira et al., 2015). Irrespective of the
303 cause, prediction of the OspB cleavage site producing the C-terminal fragment cannot be based on gel
304 migration. Tco89p is an intrinsically disordered protein and these proteins are often enriched in
305 phosphorylation sites (Miao et al., 2018). Moreover, post-translational modification is a frequent
306 regulator of intrinsically disordered proteins, so it is conceivable that TORC1 regulates its own function
307 by altering the phosphorylation state of Tco89p, consistent with a role for this protein in formation of
308 inhibitory TORC1 “body” formation during glucose and nitrogen starvation (Hughes Hallett et al.,
309 2015; Sullivan et al., 2019).

bioRxiv preprint doi: https://doi.org/10.1101/2021.09.01.458261; this version posted April 1, 2022. The copyright holder for this preprint (which was not certified by peer review) is the author/funder, who has granted bioRxiv a license to display the preprint in perpetuity. It is made available under aCC-BY 4.0 International license.

Of note, there is no obvious homolog of Tco89p in mammalian cells. However, since Tco89p is intrinsically disordered, due to the absence of structural constraints, it would be expected to have evolved rapidly and to have undergone positive selection at specific sites, resulting in the acquisition of new functions (Afanasyeva et al., 2018), leading us to postulate that the mammalian functional homolog is divergent at the sequence level. Notwithstanding this potential lack of recognizable sequence identity, our yeast OspB phenotype of sensitization to TOR inhibition is similar to our prior finding of OspB mediated sensitization to rapamycin in fibroblasts (Lu et al., 2015), bolstering the relevance of the yeast model.

The potential utility of identifying a substrate of a microbial protease in a heterologous system, as we did here for OspB, is exemplified by the work leading to the identification of the physiological ligand of the NLRP1 inflammasome. The *Bacillus anthracis* lethal factor protease efficiently cleaves a disordered linker in murine NLRP1B and rat NLRP1, releasing an arginine N-degron, degradation of which led to inflammasome activation in macrophages and pyroptotic cell death (Boyden & Dietrich, 2006; Levinsohn et al., 2012; Wickliffe et al., 2008). Anthrax is primarily a pathogen of humans, and lethal factor does not cleave the human NLRP1 homolog (Chavarría-Smith et al., 2016). Yet, these studies facilitated the recent determination that dependence on functional degradation is a conserved feature of NLRP1 activation (Chui et al., 2019; Sandstrom et al., 2019; Xu et al., 2019), and the subsequent molecular identification of enteroviral proteases as the physiological activators of the human NLRP1 inflammasome, in which cleavage of the aforementioned disordered linker generates a glycine N-degron (Robinson et al., 2020; Tsu et al., 2021). By analogy, through determination of the activity of OspB, our study provides an important insight into its substrate specificity and phenotypic impact, which will facilitate identification of mammalian substrates.

Acknowledgments

We thank Austin C. Hachey and Yang Fu for technical assistance, and Ted Powers and Nick Laribee for the gift of yeast strains. The work was supported by Department of Defense grant TS160046 (to M.B.G.), funding from the Massachusetts General Hospital Executive Committee on Research (to

bioRxiv preprint doi: https://doi.org/10.1101/2021.09.01.458261; this version posted April 1, 2022. The copyright holder for this preprint (which was not certified by peer review) is the author/funder, who has granted bioRxiv a license to display the preprint in perpetuity. It is made available under aCC-BY 4.0 International license.

M.B.G.), NIH grants T32 AI007061 and F32 AI131582 (to H.D.E.), and R01 AI064285 (to C.F.L.). The authors have no conflicts of interest.

Materials and Methods

Strains and media

All strains, plasmids and primers are listed in **Table S1**, **S2** and **S3**, respectively. *E. coli* DH10B (Grant et al., 1990) was used as the routine cloning host and was grown in Luria broth at 37 °C with agitation. *S. cerevisiae* S288C was used as the heterologous expression host to probe the roles of host proteins in the function of OspB and was routinely cultured at 30 °C in yeast extract-peptone-dextrose (YPD) broth or in synthetic selective media (MP Biomedicals) lacking histidine, uracil and/or leucine for auxotrophic selection. 1.5 % (w/v) agar was added for solid media formulations, and where appropriate, media was supplemented with 50 µg/ml ampicillin (Sigma, A9518), 2% (w/v) D-glucose (Fisher Scientific, D16-10), 2% D-(+)-raffinose (Sigma, R7630), 2% (w/v) D-galactose (VWR, 200001-176), 300 µg/ml hygromycin (Gibco, 10687010), 200 µg/ml geneticin (Sigma, A1720). For TORC1 inhibition, solid media was supplemented with 6 mM caffeine (Sigma, C0750) or 5 nM rapamycin (Sigma, 553211) unless stated otherwise. For proteasome inhibition, media was supplemented with 75 µM MG-132 (Selleck Chemicals, S2619) and 0.003% SDS. Yeast strains were transformed using the standard lithium acetate method.

Bioinformatic analyses

In silico modelling of the tertiary structure of OspB was conducted on the Phyre2 server (Kelley et al., 2015), whereas alignment with the crystal structures of $RtxA^{VC}$ (Lupardus et al., 2008) and TcdA (Pruitt et al., 2009) was achieved using the CEAlign algorithm within PyMol (Schrödinger, LLC). Protein sequences were retrieved from the non-redundant NCBI database and aligned using MUSCLE (Edgar, 2004) before manual curation to select the regions of interest.

Yeast growth assays and protein extraction

Individual yeast transformants that constitutively express *ospB* or derivatives containing point mutations were grown in synthetic selective liquid media containing 2% D-glucose. To investigate the

bioRxiv preprint doi: https://doi.org/10.1101/2021.09.01.458261; this version posted April 1, 2022. The copyright holder for this preprint (which was not certified by peer review) is the author/funder, who has granted bioRxiv a license to display the preprint in perpetuity. It is made available under aCC-BY 4.0 International license.

impact of OspB constructs on growth, yeast cells were washed and serially diluted four-fold in phosphate-buffered saline before 5 µl of each dilution were spotted on synthetic selective solid media with additives as appropriate. Assessment of protein production was done from liquid cultures. Here, subcultures were inoculated at OD_{600} 2.0 from overnight cultures and grown for two hours before harvesting for SDS-PAGE analysis using the alkaline lysis method (Kushnirov, 2000). Where construct induction was required, yeast strains were subcultured in 2% raffinose for 2 h, before supplementation with 2% galactose. Samples were harvested after four hours of protein expression. For proteasome inhibition, yeast strains were subscultured in glucose for 2 h before treatment with MG-132 or DMSO control for 3 h.

Yeast library screening

To screen for suppressors of OspB-mediated toxicity in *S. cerevisiae* by yeast gene over-expression, the strain BY4742 pAG413GPD-*ospB* was mated with the haploid GST-fusion yeast over-expression library (Dharmacon, YSC4423) on YPD. The resulting diploids were selected by plating on non-inducing synthetic selective media containing 2% D-glucose. The screen was conducted by spotting in quadruplicate on inducing synthetic selective solid media containing 2% D-galactose and 6 mM caffeine. All steps in the screen were conducted in an automated manner as described previously (Slagowski et al., 2008). Suppressors were classified as strains which displayed qualitatively moderate to robust growth of all four spots on the caffeine plate four days after pinning. To screen for *S. cerevisiae* host factors required for OspB-dependent growth inhibition, we screened the MAT**a** haploid deletion library (Horizon, YSC1053) as previously described (Kramer et al., 2007), but with transformation of the plasmid pAG413GAL-*ospB* and assessment of growth on synthetic selective solid media containing 2% D-galactose and 6 mM caffeine after 3 days.

Cell culture and transfection

HEK293T (ATCC) and mouse embryonic fibroblast cells (Lu et al., 2015) were maintained in Dulbecco's modified Eagle medium (DMEM) (Gibco) supplemented with 10% (v/v) fetal bovine serum

bioRxiv preprint doi: https://doi.org/10.1101/2021.09.01.458261; this version posted April 1, 2022. The copyright holder for this preprint (which was not certified by peer review) is the author/funder, who has granted bioRxiv a license to display the preprint in perpetuity. It is made available under aCC-BY 4.0 International license.

at 37 °C with 5% CO_2. Cells were transfected with plasmids using FuGENE6 (Promega) according to the manufacturer's instructions, and experimental samples were analyzed 24-48 h after transfection.

SDS-PAGE and immunoblotting

For immunoblot analysis, protein samples were separated by SDS-PAGE, transferred to nitrocellulose membranes and detected by western blot analysis using standard procedures. The antibodies used were peroxidase-conjugated anti-β-actin (Sigma, A3854; diluted to 1:10 000), anti-α-tubulin (Santa Cruz, sc-53030; diluted to 1:1000), anti-FLAG (Sigma, F3165; diluted to 1:1000), anti-myc (EMD Millipore 05-724; diluted to 1:1000), anti-HA (Biolegend, 901501, diluted to 1:1000) and anti-OspB (diluted to 1:10 000). The rabbit anti-OspB antibody was generated (Covance Inc.) against a 14-mer peptide of OspB located 18 residues from the C-terminus.

References

Afanasyeva, A., Bockwoldt, M., Cooney, C. R., Heiland, I., & Gossmann, T. I. (2018). Human long intrinsically disordered protein regions are frequent targets of positive selection. *Genome Research*, *28*(7), 975–982. https://doi.org/10.1101/gr.232645.117

Agaisse, H. (2016). Molecular and Cellular Mechanisms of *Shigella flexneri* Dissemination. *Frontiers in Cellular and Infection Microbiology*, *6*(March), 29. https://doi.org/10.3389/fcimb.2016.00029

Ambrosi, C., Pompili, M., Scribano, D., Limongi, D., Petrucca, A., Cannavacciuolo, S., Schippa, S., Zagaglia, C., Grossi, M., & Nicoletti, M. (2015). The *Shigella flexneri* OspB effector: an early immunomodulator. *International Journal of Medical Microbiology*, *305*(1), 75–84. https://doi.org/10.1016/j.ijmm.2014.11.004

Anderson, D. M., Schmalzer, K. M., Sato, H., Casey, M., Terhune, S. S., Haas, A. L., Feix, J. B., & Frank, D. W. (2011). Ubiquitin and ubiquitin-modified proteins activate the *Pseudomonas aeruginosa* T3SS cytotoxin, ExoU. *Molecular Microbiology*, *82*(6), 1454–1467. https://doi.org/10.1111/j.1365-2958.2011.07904.x

Ashida, H., Sasakawa, C., & Suzuki, T. (2020). A unique bacterial tactic to circumvent the cell death crosstalk induced by blockade of caspase-8. *The EMBO Journal*, 1–16. https://doi.org/10.15252/embj.2020104469

Baker, R. T., & Varshavsky, A. (1995). Yeast N-terminal amidase: a new enzyme and component of the N-end rule pathway. *The Journal of Biological Chemistry*, *270*(20), 12065–12074. https://doi.org/10.1074/JBC.270.20.12065

Bartel, B., Wünning, I., & Varshavsky, A. (1990). The recognition component of the N-end rule pathway. *The EMBO Journal*, *9*(10), 3179–3189. https://doi.org/10.1002/j.1460-2075.1990.tb07516.x

Binda, M., Péli-Gulli, M.-P., Bonfils, G., Panchaud, N., Urban, J., Sturgill, T. W., Loewith, R., & De

bioRxiv preprint doi: https://doi.org/10.1101/2021.09.01.458261; this version posted April 1, 2022. The copyright holder for this preprint (which was not certified by peer review) is the author/funder, who has granted bioRxiv a license to display the preprint in perpetuity. It is made available under aCC-BY 4.0 International license.

Virgilio, C. (2009). The Vam6 GEF controls TORC1 by activating the EGO complex. *Molecular Cell*, *35*(5), 563–573. https://doi.org/10.1016/j.molcel.2009.06.033

Boyden, E. D., & Dietrich, W. F. (2006). *Nalp1b* controls mouse macrophage susceptibility to anthrax lethal toxin. *Nature Genetics*, *38*(2), 240–244. https://doi.org/10.1038/ng1724

Brown, N. F., & Finlay, B. (2011). Potential origins and horizontal transfer of type III secretion systems and effectors. *Mobile Genetic Elements*, *1*(2), 118–121. https://doi.org/10.4161/mge.1.2.16733

Burnaevskiy, N., Fox, T. G., Plymire, D. A., Ertelt, J. M., Weigele, B. A., Selyunin, A. S., Way, S. S., Patrie, S. M., & Alto, N. M. (2013). Proteolytic elimination of *N*-myristoyl modifications by the *Shigella* virulence factor IpaJ. *Nature*, *496*(7443), 106–109. https://doi.org/10.1038/nature12004

Burnaevskiy, N., Peng, T., Reddick, L. E., Hang, H. C., & Alto, N. M. (2015). Myristoylome profiling reveals a concerted mechanism of ARF GTPase deacylation by the bacterial protease IpaJ. *Molecular Cell*, *58*(1), 110–122. https://doi.org/10.1016/j.molcel.2015.01.040

Calder, T., Kinch, L. N., Fernandez, J., Salomon, D., Grishin, N. V., & Orth, K. (2014). *Vibrio type* III effector VPA1380 is related to the cysteine protease domain of large bacterial toxins. *PLoS ONE*, *9*(8), e104387. https://doi.org/10.1371/journal.pone.0104387

Carayol, N., & Tran Van Nhieu, G. (2013). The inside story of *Shigella* invasion of intestinal epithelial cells. *Cold Spring Harbor Perspectives in Medicine*, *3*(10), a016717. https://doi.org/10.1101/cshperspect.a016717

Chavarría-Smith, J., Mitchell, P. S., Ho, A. M., Daugherty, M. D., & Vance, R. E. (2016). Functional and Evolutionary Analyses Identify Proteolysis as a General Mechanism for NLRP1 Inflammasome Activation. *PLoS Pathogens*, *12*(12), e1006052. https://doi.org/10.1371/journal.ppat.1006052

Chen, S.-J., Wu, X., Wadas, B., Oh, J.-H., & Varshavsky, A. (2017). An N-end rule pathway that recognizes proline and destroys gluconeogenic enzymes. *Science*, *355*(6323). https://doi.org/10.1126/science.aal3655

Chui, A. J., Okondo, M. C., Rao, S. D., Gai, K., Griswold, A. R., Johnson, D. C., Ball, D. P., Taabazuing, C. Y., Orth, E. L., Vittimberga, B. A., & Bachovchin, D. A. (2019). N-terminal degradation activates the NLRP1B inflammasome. *Science*, *1208*(March), 317826. https://doi.org/10.1126/science.aau1208

Coaker, G., Falick, A., & Staskawicz, B. J. (2005). Activation of a phytopathogenic bacterial effector protein by a eukaryotic cyclophilin. *Science*, *308*(5721), 548–550. https://doi.org/10.1126/science.1108633

Dohmen, R. J., Madura, K., Bartel, B., & Varshavsky, A. (1991). The N-end rule is mediated by the UBC2(RAD6) ubiquitin-conjugating enzyme. *Proceedings of the National Academy of Sciences of the United States of America*, *88*(16), 7351–7355. https://doi.org/10.1073/pnas.88.16.7351

Drum, C. L., Yan, S.-Z., Bard, J., Shen, Y.-Q., Lu, D., Soelaiman, S., Grabarek, Z., Bohm, A., & Tang, W.-J. (2002). Structural basis for the activation of anthrax adenylyl cyclase exotoxin by calmodulin. *Nature*, *415*(6870), 396–402. https://doi.org/10.1038/415396a

Dubouloz, F., Deloche, O., Wanke, V., Cameroni, E., & De Virgilio, C. (2005). The TOR and EGO Protein Complexes Orchestrate Microautophagy in Yeast. *Molecular Cell*, *19*(1), 15–26.

bioRxiv preprint doi: https://doi.org/10.1101/2021.09.01.458261; this version posted April 1, 2022. The copyright holder for this preprint (which was not certified by peer review) is the author/funder, who has granted bioRxiv a license to display the preprint in perpetuity. It is made available under aCC-BY 4.0 International license.

460 https://doi.org/10.1016/j.molcel.2005.05.020

461 Edgar, R. C. (2004). MUSCLE: multiple sequence alignment with high accuracy and high throughput.
462 *Nucleic Acids Research*, *32*(5), 1792–1797. https://doi.org/10.1093/nar/gkh340

463 Egerer, M., Giesemann, T., Jank, T., Satchell, K. J. F., & Aktories, K. (2007). Auto-catalytic cleavage
464 of *Clostridium difficile* toxins A and B depends on cysteine protease activity. *The Journal of*
465 *Biological Chemistry*, *282*(35), 25314–25321. https://doi.org/10.1074/jbc.M703062200

466 Egerer, M., & Satchell, K. J. F. (2010). Inositol Hexakisphosphate-Induced Autoprocessing of Large
467 Bacterial Protein Toxins. *PLoS Pathogens*, *6*(7), e1000942.
468 https://doi.org/10.1371/journal.ppat.1000942

469 Eisenreich, W., Heesemann, J., Rudel, T., & Goebel, W. (2013). Metabolic host responses to infection
470 by intracellular bacterial pathogens. *Frontiers in Cellular and Infection Microbiology*, *3*(JUL), 1–22.
471 https://doi.org/10.3389/fcimb.2013.00024

472 Fukazawa, A., Alonso, C., Kurachi, K., Gupta, S., Lesser, C. F., McCormick, B. A., & Reinecker, H.-
473 C. (2008). GEF-H1 mediated control of NOD1 dependent NF-κB activation by *Shigella* effectors.
474 *PLoS Pathogens*, *4*(11), e1000228. https://doi.org/10.1371/journal.ppat.1000228

475 Fullner, K. J., & Mekalanos, J. J. (2000). *In vivo* covalent cross-linking of cellular actin by the *Vibrio*
476 *cholerae* RTX toxin. *The EMBO Journal*, *19*(20), 5315–5323.
477 https://doi.org/10.1093/emboj/19.20.5315

478 Gonda, D. K., Bachmair, A., Wünning, I., Tobias, J. W., Lane, W. S., & Varshavsky, A. (1989).
479 Universality and Structure of the N-end Rule. *Journal of Biological Chemistry*, *264*(28), 16700–
480 16712. https://doi.org/10.1016/S0021-9258(19)84762-2

481 González, A., & Hall, M. N. (2017). Nutrient sensing and TOR signaling in yeast and mammals. *The*
482 *EMBO Journal*, *36*(4), 397–408. https://doi.org/10.15252/embj.201696010

483 Grant, S. G. N., Jessee, J., Bloom, F. R., & Hanahan, D. (1990). Differential plasmid rescue from
484 transgenic mouse DNAs into *Escherichia coli* methylation-restriction mutants. *Proceedings of the*
485 *National Academy of Sciences*, *87*(12), 4645–4649. https://doi.org/10.1073/pnas.87.12.4645

486 Huber, A., Bodenmiller, B., Uotila, A., Stahl, M., Wanka, S., Gerrits, B., Aebersold, R., & Loewith,
487 R. (2009). Characterization of the rapamycin-sensitive phosphoproteome reveals that Sch9 is a central
488 coordinator of protein synthesis. *Genes & Development*, *23*(16), 1929–1943.
489 https://doi.org/10.1101/gad.532109

490 Hughes Hallett, J. E., Luo, X., & Capaldi, A. P. (2014). State Transitions in the TORC1 Signaling
491 Pathway and Information Processing in Saccharomyces cerevisiae. *Genetics*, *198*(2), 773–786.
492 https://doi.org/10.1534/genetics.114.168369

493 Hughes Hallett, J. E., Luo, X., & Capaldi, A. P. (2015). Snf1/AMPK promotes the formation of
494 Kog1/Raptor-bodies to increase the activation threshold of TORC1 in budding yeast. *ELife*,
495 *4*(OCTOBER2015), 1–19. https://doi.org/10.7554/eLife.09181

496 Hwang, W. W., Venkatasubrahmanyam, S., Ianculescu, A. G., Tong, A., Boone, C., & Madhani, H.
497 D. (2003). A conserved RING finger protein required for histone H2B monoubiquitination and cell
498 size control. *Molecular Cell*, *11*(1), 261–266. http://www.ncbi.nlm.nih.gov/pubmed/12535538

bioRxiv preprint doi: https://doi.org/10.1101/2021.09.01.458261; this version posted April 1, 2022. The copyright holder for this preprint (which was not certified by peer review) is the author/funder, who has granted bioRxiv a license to display the preprint in perpetuity. It is made available under aCC-BY 4.0 International license.

Just, I., Selzer, J., Wilm, M., von Eichel-Streiber, C., Mann, M., & Aktories, K. (1995). Glucosylation of Rho proteins by *Clostridium difficile* toxin B. *Nature*, *375*(6531), 500–503. https://doi.org/10.1038/375500a0

Kelley, L. A., Mezulis, S., Yates, C. M., Wass, M. N., & Sternberg, M. J. E. (2015). The Phyre2 web portal for protein modeling, prediction and analysis. *Nature Protocols*, *10*(6), 845–858. https://doi.org/10.1038/nprot.2015-053

Khalil, I. A., Troeger, C., Blacker, B. F., Rao, P. C., Brown, A., Atherly, D. E., Brewer, T. G., Engmann, C. M., Houpt, E. R., Kang, G., Kotloff, K. L., Levine, M. M., Luby, S. P., MacLennan, C. A., Pan, W. K., Pavlinac, P. B., Platts-Mills, J. A., Qadri, F., Riddle, M. S., … Reiner, R. C. (2018). Morbidity and mortality due to *Shigella* and enterotoxigenic *Escherichia coli* diarrhoea: the Global Burden of Disease Study 1990-2016. *The Lancet Infectious Diseases*, *18*(11), 1229–1240. https://doi.org/10.1016/S1473-3099(18)30475-4

Kim, A., & Cunningham, K. W. (2015). A LAPF/phafin1-like protein regulates TORC1 and lysosomal membrane permeabilization in response to endoplasmic reticulum membrane stress. *Molecular Biology of the Cell*, *26*(25), 4631–4645. https://doi.org/10.1091/mbc.E15-08-0581

Kim, J.-M., Seok, O.-H., Ju, S., Heo, J.-E., Yeom, J., Kim, D.-S., Yoo, J.-Y., Varshavsky, A., Lee, C., & Hwang, C.-S. (2018). Formyl-methionine as an N-degron of a eukaryotic N-end rule pathway. *Science*, *362*(6418), eaat0174. https://doi.org/10.1126/science.aat0174

Kramer, R. W., Slagowski, N. L., Eze, N. A., Giddings, K. S., Morrison, M. F., Siggers, K. A., Starnbach, M. N., & Lesser, C. F. (2007). Yeast functional genomic screens lead to identification of a role for a bacterial effector in innate immunity regulation. *PLoS Pathogens*, *3*(2), e21. https://doi.org/10.1371/journal.ppat.0030021

Kushnirov, V. V. (2000). Rapid and reliable protein extraction from yeast. *Yeast*, *16*(9), 857–860. https://doi.org/10.1002/1097-0061(20000630)16:9<857::AID-YEA561>3.0.CO;2-B

Levinsohn, J. L., Newman, Z. L., Hellmich, K. A., Fattah, R., Getz, M. A., Liu, S., Sastalla, I., Leppla, S. H., & Moayeri, M. (2012). Anthrax Lethal Factor Cleavage of Nlrp1 Is Required for Activation of the Inflammasome. *PLoS Pathogens*, *8*(3), e1002638. https://doi.org/10.1371/journal.ppat.1002638

Li, H., Xu, H., Zhou, Y., Zhang, J., Long, C., Li, S., Chen, S., Zhou, J. M., & Shao, F. (2007). The phosphothreonine lyase activity of a bacterial type III effector family. *Science*, *315*(5814), 1000–1003. https://doi.org/10.1126/science.1138960

Li, Z., Liu, W., Fu, J., Cheng, S., Xu, Y., Wang, Z., Liu, X., Shi, X., Liu, Y., Qi, X., Liu, X., Ding, J., & Shao, F. (2021). *Shigella* evades pyroptosis by arginine ADP-riboxanation of caspase-11. *Nature*, *599*(7884), 290–295. https://doi.org/10.1038/s41586-021-04020-1

Liu, W., Zhou, Y., Peng, T., Zhou, P., Ding, X., Li, Z., Zhong, H., Xu, Y., Chen, S., Hang, H. C., & Shao, F. (2018). N^{ε}-fatty acylation of multiple membrane-associated proteins by *Shigella* IcsB effector to modulate host function. *Nature Microbiology*, *3*(9), 996–1009. https://doi.org/10.1038/s41564-018-0215-6

Lu, R., Herrera, B. B., Eshleman, H. D., Fu, Y., Bloom, A., Li, Z., Sacks, D. B., & Goldberg, M. B. (2015). *Shigella* Effector OspB Activates mTORC1 in a Manner That Depends on IQGAP1 and Promotes Cell Proliferation. *PLoS Pathogens*, *11*(10), e1005200. https://doi.org/10.1371/journal.ppat.1005200

bioRxiv preprint doi: https://doi.org/10.1101/2021.09.01.458261; this version posted April 1, 2022. The copyright holder for this preprint (which was not certified by peer review) is the author/funder, who has granted bioRxiv a license to display the preprint in perpetuity. It is made available under aCC-BY 4.0 International license.

Lupardus, P. J., Shen, A., Bogyo, M., & Garcia, K. C. (2008). Small molecule-induced allosteric activation of the *Vibrio cholerae* RTX cysteine protease domain. *Science*, *322*(5899), 265–268. https://doi.org/10.1126/science.1162403

Melnykov, A., Chen, S.-J., & Varshavsky, A. (2019). Gid10 as an alternative N-recognin of the Pro/N-degron pathway. *Proceedings of the National Academy of Sciences*, *116*(32), 15914–15923. https://doi.org/10.1073/pnas.1908304116

Miao, Y., Tipakornsaowapak, T., Zheng, L., Mu, Y., & Lewellyn, E. (2018). Phospho-regulation of intrinsically disordered proteins for actin assembly and endocytosis. *The FEBS Journal*, *285*(15), 2762–2784. https://doi.org/10.1111/febs.14493

Mittal, R., Peak-Chew, S. Y., Sade, R. S., Vallis, Y., & McMahon, H. T. (2010). The acetyltransferase activity of the bacterial toxin YopJ of *Yersinia* is activated by eukaryotic host cell inositol hexakisphosphate. *The Journal of Biological Chemistry*, *285*(26), 19927–19934. https://doi.org/10.1074/jbc.M110.126581

Mulugu, S., Bai, W., Fridy, P. C., Bastidas, R. J., Otto, J. C., Dollins, D. E., Haystead, T. A., Ribeiro, A. A., & York, J. D. (2007). A conserved family of enzymes that phosphorylate inositol hexakisphosphate. *Science*, *316*(5821), 106–109. https://doi.org/10.1126/science.1139099

Niebuhr, K., Giuriato, S., Pedron, T., Philpott, D. J., Gaits, F., Sable, J., Sheetz, M. P., Parsot, C., Sansonetti, P. J., & Payrastre, B. (2002). Conversion of PtdIns(4,5)P_2 into PtdIns(5)P by the *S. flexneri* effector IpgD reorganizes host cell morphology. *The EMBO Journal*, *21*(19), 5069–5078. https://doi.org/10.1093/emboj/cdf522

Oliveira, A. P., Ludwig, C., Zampieri, M., Weisser, H., Aebersold, R., & Sauer, U. (2015). Dynamic phosphoproteomics reveals TORC1-dependent regulation of yeast nucleotide and amino acid biosynthesis. *Science Signaling*, *8*(374), rs4. https://doi.org/10.1126/scisignal.2005768

Prochazkova, K., & Satchell, K. J. F. (2008). Structure-function analysis of inositol hexakisphosphate-induced autoprocessing of the *Vibrio cholerae* multifunctional autoprocessing RTX toxin. *The Journal of Biological Chemistry*, *283*(35), 23656–23664. https://doi.org/10.1074/jbc.M803334200

Pruitt, R. N., Chagot, B., Cover, M., Chazin, W. J., Spiller, B., & Lacy, D. B. (2009). Structure-function analysis of inositol hexakisphosphate-induced autoprocessing in *Clostridium difficile* toxin A. *The Journal of Biological Chemistry*, *284*(33), 21934–21940. https://doi.org/10.1074/jbc.M109.018929

Reineke, J., Tenzer, S., Rupnik, M., Koschinski, A., Hasselmayer, O., Schrattenholz, A., Schild, H., & von Eichel-Streiber, C. (2007). Autocatalytic cleavage of Clostridium difficile toxin B. *Nature*, *446*(7134), 415–419. https://doi.org/10.1038/nature05622

Reinke, A., Anderson, S., McCaffery, J. M., Yates, J., Aronova, S., Chu, S., Fairclough, S., Iverson, C., Wedaman, K. P., & Powers, T. (2004). TOR complex 1 includes a novel component, Tco89p (YPL180w), and cooperates with Ssd1p to maintain cellular integrity in *Saccharomyces cerevisiae*. *The Journal of Biological Chemistry*, *279*(15), 14752–14762. https://doi.org/10.1074/jbc.M313062200

Reinke, A., Chen, J. C.-Y., Aronova, S., & Powers, T. (2006). Caffeine targets TOR complex I and provides evidence for a regulatory link between the FRB and kinase domains of Tor1p. *The Journal of Biological Chemistry*, *281*(42), 31616–31626. https://doi.org/10.1074/jbc.M603107200

bioRxiv preprint doi: https://doi.org/10.1101/2021.09.01.458261; this version posted April 1, 2022. The copyright holder for this preprint (which was not certified by peer review) is the author/funder, who has granted bioRxiv a license to display the preprint in perpetuity. It is made available under aCC-BY 4.0 International license.

583 Richter-Ruoff, B., Heinemeyer, W., & Wolf, D. H. (1992). The proteasome/multicatalytic-
584 multifunctional proteinase. *In vivo* function in the ubiquitin-dependent N-end rule pathway of protein
585 degradation in eukaryotes. *FEBS Letters*, *302*(2), 192–196. https://doi.org/10.1016/0014-
586 5793(92)80438-M

587 Robinson, K. S., Teo, D. E. T., Tan, K. Sen, Toh, G. A., Ong, H. H., Lim, C. K., Lay, K., Au, B. V.,
588 Lew, T. S., Chu, J. J. H., Chow, V. T. K., Wang, D. Y., Zhong, F. L., & Reversade, B. (2020).
589 Enteroviral 3C protease activates the human NLRP1 inflammasome in airway epithelia. *Science*,
590 *370*(6521), eaay2002. https://doi.org/10.1126/science.aay2002

591 Rohde, J. R., Breitkreutz, A., Chenal, A., Sansonetti, P. J., & Parsot, C. (2007). Type III secretion
592 effectors of the IpaH family are E3 ubiquitin ligases. *Cell Host and Microbe*, *1*(1), 77–83.
593 https://doi.org/10.1016/j.chom.2007.02.002

594 Saiardi, A., Sciambi, C., McCaffery, J. M., Wendland, B., & Snyder, S. H. (2002). Inositol
595 pyrophosphates regulate endocytic trafficking. *Proceedings of the National Academy of Sciences*,
596 *99*(22), 14206–14211. https://doi.org/10.1073/pnas.212527899

597 Sandstrom, A., Mitchell, P. S., Goers, L., Mu, E. W., Lesser, C. F., & Vance, R. E. (2019). Functional
598 degradation: A mechanism of NLRP1 inflammasome activation by diverse pathogen enzymes.
599 *Science*, *364*(6435), 1–13. https://doi.org/10.1126/science.aau1330

600 Savidge, T. C., Urvil, P., Oezguen, N., Ali, K., Choudhury, A., Acharya, V., Pinchuk, I., Torres, A.
601 G., English, R. D., Wiktorowicz, J. E., Loeffelholz, M., Kumar, R., Shi, L., Nie, W., Braun, W.,
602 Herman, B., Hausladen, A., Feng, H., Stamler, J. S., & Pothoulakis, C. (2011). Host *S*-nitrosylation
603 inhibits clostridial small molecule-activated glucosylating toxins. *Nature Medicine*, *17*(9), 1136–1141.
604 https://doi.org/10.1038/nm.2405

605 Sheahan, K., Cordero, C. L., & Satchell, K. J. F. (2007). Autoprocessing of the *Vibrio cholerae* RTX
606 toxin by the cysteine protease domain. *The EMBO Journal*, *26*(10), 2552–2561.
607 https://doi.org/10.1038/sj.emboj.7601700

608 Shen, A., Lupardus, P. J., Albrow, V. E., Guzzetta, A., Powers, J. C., Garcia, K. C., & Bogyo, M.
609 (2009). Mechanistic and structural insights into the proteolytic activation of *Vibrio cholerae* MARTX
610 toxin. *Nature Chemical Biology*, *5*(7), 469–478. https://doi.org/10.1038/nchembio.178

611 Slagowski, N. L., Kramer, R. W., Morrison, M. F., LaBaer, J., & Lesser, C. F. (2008). A Functional
612 Genomic Yeast Screen to Identify Pathogenic Bacterial Proteins. *PLoS Pathogens*, *4*(1).
613 https://doi.org/10.1371/journal.ppat.0040009

614 Sopko, R., Huang, D., Preston, N., Chua, G., Papp, B., Kafadar, K., Snyder, M., Oliver, S. G., Cyert,
615 M., Hughes, T. R., Boone, C., & Andrews, B. (2006). Mapping pathways and phenotypes by
616 systematic gene overexpression. *Molecular Cell*, *21*(3), 319–330.
617 https://doi.org/10.1016/j.molcel.2005.12.011

618 Sreelatha, A., Nolan, C., Park, B. C., Pawłowski, K., Tomchick, D. R., & Tagliabracci, V. S. (2020).
619 A *Legionella* effector kinase is activated by host inositol hexakisphosphate. *The Journal of Biological*
620 *Chemistry*, *1*, jbc.RA120.013067. https://doi.org/10.1074/jbc.RA120.013067

621 Sullivan, A., Wallace, R. L., Wellington, R., Luo, X., & Capaldi, A. P. (2019). Multilayered
622 regulation of TORC1-body formation in budding yeast. *Molecular Biology of the Cell*, *30*(3), 400–
623 410. https://doi.org/10.1091/mbc.E18-05-0297

bioRxiv preprint doi: https://doi.org/10.1101/2021.09.01.458261; this version posted April 1, 2022. The copyright holder for this preprint (which was not certified by peer review) is the author/funder, who has granted bioRxiv a license to display the preprint in perpetuity. It is made available under aCC-BY 4.0 International license.

624 Tanigawa, M., Yamamoto, K., Nagatoishi, S., Nagata, K., Noshiro, D., Noda, N. N., Tsumoto, K., &
625 Maeda, T. (2021). A glutamine sensor that directly activates TORC1. *Communications Biology*, *4*(1),
626 1093. https://doi.org/10.1038/s42003-021-02625-w

627 Tsu, B. V., Beierschmitt, C., Ryan, A. P., Agarwal, R., Mitchell, P. S., & Daugherty, M. D. (2021).
628 Diverse viral proteases activate the NLRP1 inflammasome. *ELife*, *10*(9), 1689–1699.
629 https://doi.org/10.7554/eLife.60609

630 Tyson, G. H., & Hauser, A. R. (2013). Phosphatidylinositol 4,5-Bisphosphate Is a Novel Coactivator
631 of the *Pseudomonas aeruginosa* Cytotoxin ExoU. *Infection and Immunity*, *81*(8), 2873–2881.
632 https://doi.org/10.1128/IAI.00414-13

633 Ukai, H., Araki, Y., Kira, S., Oikawa, Y., May, A. I., & Noda, T. (2018). Gtr/Ego-independent
634 TORC1 activation is achieved through a glutamine-sensitive interaction with Pib2 on the vacuolar
635 membrane. *PLoS Genetics*, *14*(4), e1007334. https://doi.org/10.1371/journal.pgen.1007334

636 Varshavsky, A. (2019). N-degron and C-degron pathways of protein degradation. *Proceedings of the*
637 *National Academy of Sciences of the United States of America*, *116*(2), 358–366.
638 https://doi.org/10.1073/pnas.1816596116

639 Wickliffe, K. E., Leppla, S. H., & Moayeri, M. (2008). Killing of macrophages by anthrax lethal
640 toxin: involvement of the N-end rule pathway. *Cellular Microbiology*, *10*(6), 1352–1362.
641 https://doi.org/10.1111/j.1462-5822.2008.01131.x

642 Wood, A., Krogan, N. J., Dover, J., Schneider, J., Heidt, J., Boateng, M. A., Dean, K., Golshani, A.,
643 Zhang, Y., Greenblatt, J. F., Johnston, M., & Shilatifard, A. (2003). Bre1, an E3 ubiquitin ligase
644 required for recruitment and substrate selection of Rad6 at a promoter. *Molecular Cell*, *11*(1), 267–
645 274. http://www.ncbi.nlm.nih.gov/pubmed/12535539

646 Xu, H., Shi, J., Gao, H., Liu, Y., Yang, Z., Shao, F., & Dong, N. (2019). The N-end rule ubiquitin
647 ligase UBR2 mediates NLRP1B inflammasome activation by anthrax lethal toxin. *The EMBO*
648 *Journal*, *38*(13), 1–11. https://doi.org/10.15252/embj.2019101996

649 Yuan, W., Guo, S., Gao, J., Zhong, M., Yan, G., Wu, W., Chao, Y., & Jiang, Y. (2017). General
650 Control Nonderepressible 2 (GCN2) Kinase Inhibits Target of Rapamycin Complex 1 in Response to
651 Amino Acid Starvation in *Saccharomyces cerevisiae*. *Journal of Biological Chemistry*, *292*(7), 2660–
652 2669. https://doi.org/10.1074/jbc.M116.772194

653 Zhang, L., Ding, X., Cui, J., Xu, H., Chen, J., Gong, Y.-N., Hu, L., Zhou, Y., Ge, J., Lu, Q., Liu, L.,
654 Chen, S., & Shao, F. (2012). Cysteine methylation disrupts ubiquitin-chain sensing in NF-κB
655 activation. *Nature*, *481*(7380), 204–208. https://doi.org/10.1038/nature10690

656 Zurawski, D. V., Mumy, K. L., Faherty, C. S., McCormick, B. A., & Maurelli, A. T. (2009). *Shigella*
657 *flexneri* type III secretion system effectors OspB and OspF target the nucleus to downregulate the host
658 inflammatory response *via* interactions with retinoblastoma protein. *Molecular Microbiology*, *71*(2),
659 350–368. https://doi.org/10.1111/j.1365-2958.2008.06524.x

660

bioRxiv preprint doi: https://doi.org/10.1101/2021.09.01.458261; this version posted April 1, 2022. The copyright holder for this preprint (which was not certified by peer review) is the author/funder, who has granted bioRxiv a license to display the preprint in perpetuity. It is made available under aCC-BY 4.0 International license.

661 # Figures

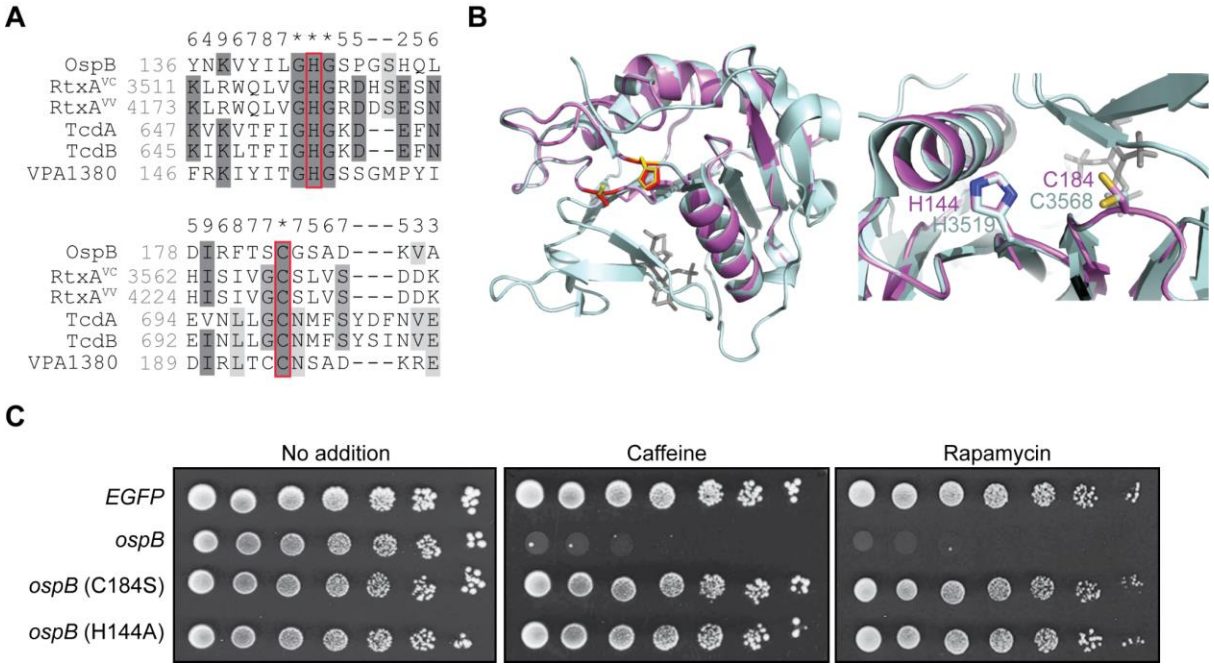

662

663 **FIGURE 1: OspB possesses a predicted cysteine protease catalytic dyad.**

664 (A) Multiple sequence alignment of OspB with the catalytic residues of the cysteine protease
665 domains of RtxA from *V. cholerae* (RtxA^{VC}) and *V. vulnificus* (RtxA^{VV}), *C. difficile* TcdA and
666 TcdB, and the OspB ortholog VPA1380 from *V. parahaemolyticus*. Red boxes indicate
667 catalytic residues of the cysteine protease domains and the aligned putative catalytic residues
668 of OspB. Darkness of gray shading reflects the conservation of individual residues, and the
669 numbers above the alignment score the conservation at each position. Asterisks denote full
670 conservation among the aligned sequences.

671 (B) Cartoon depiction of a tertiary structure model of OspB (violet) on the CPD of RtxA^{VC} (*left*
672 *panel*; PDB: 3EEB) (pale cyan). In the left panel, the catalytic residues of the cysteine protease
673 domain are denoted by yellow sticks, with the putative catalytic residues of OspB shown as red
674 sticks. The inositol hexakisphosphate cofactor in the RtxA^{VC} cysteine protease domain structure
675 is shown in dark gray. In the right panel, an enlarged and rotated view shows the active site,
676 highlighting the superposition of the putative OspB catalytic residues with those of the cysteine
677 protease domain, labelled according to the color of the cartoon.

bioRxiv preprint doi: https://doi.org/10.1101/2021.09.01.458261; this version posted April 1, 2022. The copyright holder for this preprint (which was not certified by peer review) is the author/funder, who has granted bioRxiv a license to display the preprint in perpetuity. It is made available under aCC-BY 4.0 International license.

(C) Growth of yeast strains expressing *ospB* constructs or an *EGFP* control. Serial dilutions were spotted on media either without additives or supplemented with the TORC1 inhibitors caffeine or rapamycin ($n = 3$).

bioRxiv preprint doi: https://doi.org/10.1101/2021.09.01.458261; this version posted April 1, 2022. The copyright holder for this preprint (which was not certified by peer review) is the author/funder, who has granted bioRxiv a license to display the preprint in perpetuity. It is made available under aCC-BY 4.0 International license.

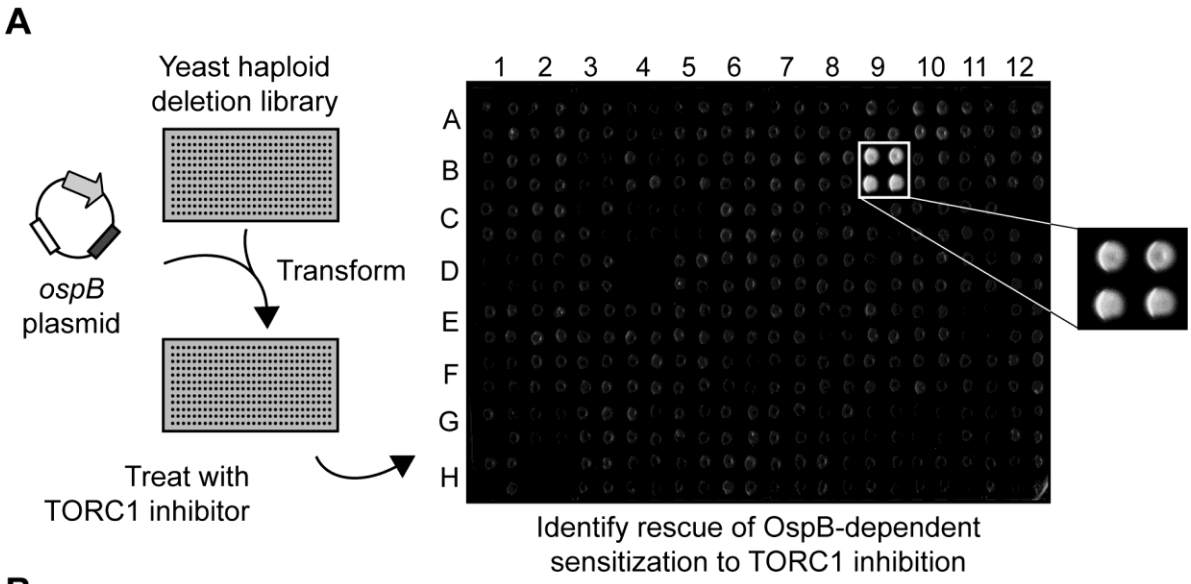

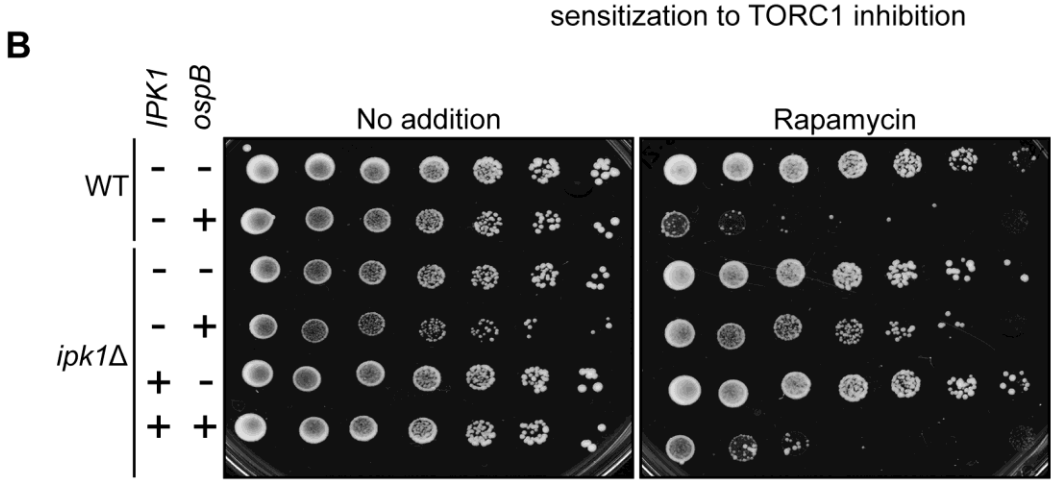

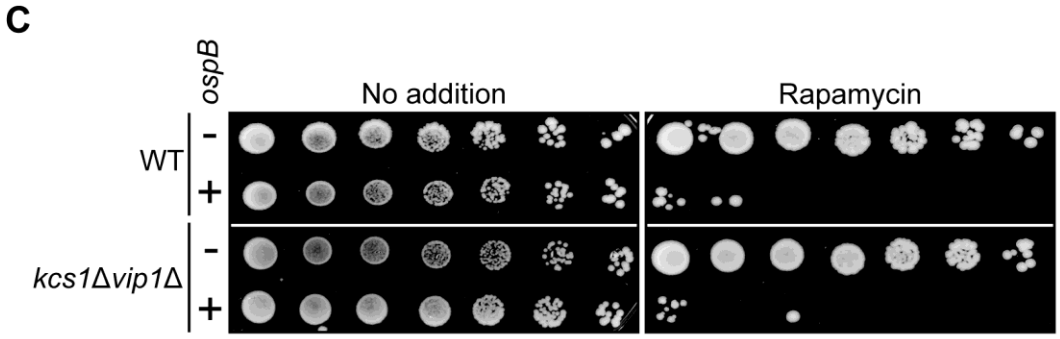

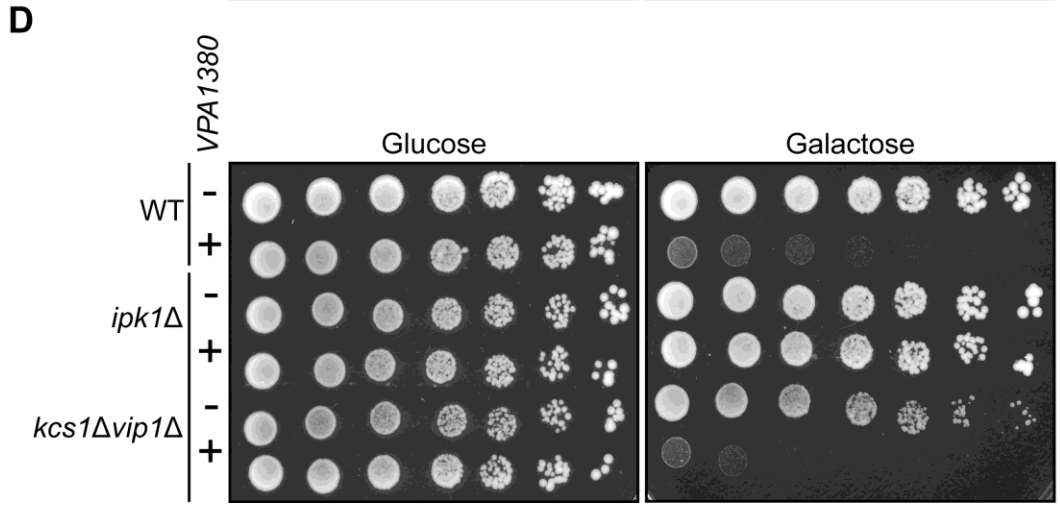

bioRxiv preprint doi: https://doi.org/10.1101/2021.09.01.458261; this version posted April 1, 2022. The copyright holder for this preprint (which was not certified by peer review) is the author/funder, who has granted bioRxiv a license to display the preprint in perpetuity. It is made available under aCC-BY 4.0 International license.

FIGURE 2: Inhibition of yeast growth by OspB-family effectors requires inositol hexakisphosphate.

(A) Schematic of the deletion library screen designed to identify yeast host factors required for OspB-mediated growth inhibition in the presence of caffeine. An example of a quadruplicate-spotted output plate is shown, with one hit magnified.

(B) Growth of yeast strains expressing *ospB* constructs or vector control in the presence or absence of *IPK1*. Serial dilutions were spotted on media with or without rapamycin.

(C) Growth of yeast strains expressing *ospB* constructs or vector control in the presence or absence of both genes encoding the IP_6 kinases Kcs1p and Vip1p. Serial dilutions were spotted on media with or without rapamycin.

(D) Growth of yeast strains expressing *VPA1380* or vector control in the WT, *ipk1*Δ, and *kcs1*Δ*vip1*Δ backgrounds. Serial dilutions were spotted on media repressing (glucose) or inducing (galactose) *VPA1380* construct expression.

bioRxiv preprint doi: https://doi.org/10.1101/2021.09.01.458261; this version posted April 1, 2022. The copyright holder for this preprint (which was not certified by peer review) is the author/funder, who has granted bioRxiv a license to display the preprint in perpetuity. It is made available under aCC-BY 4.0 International license.

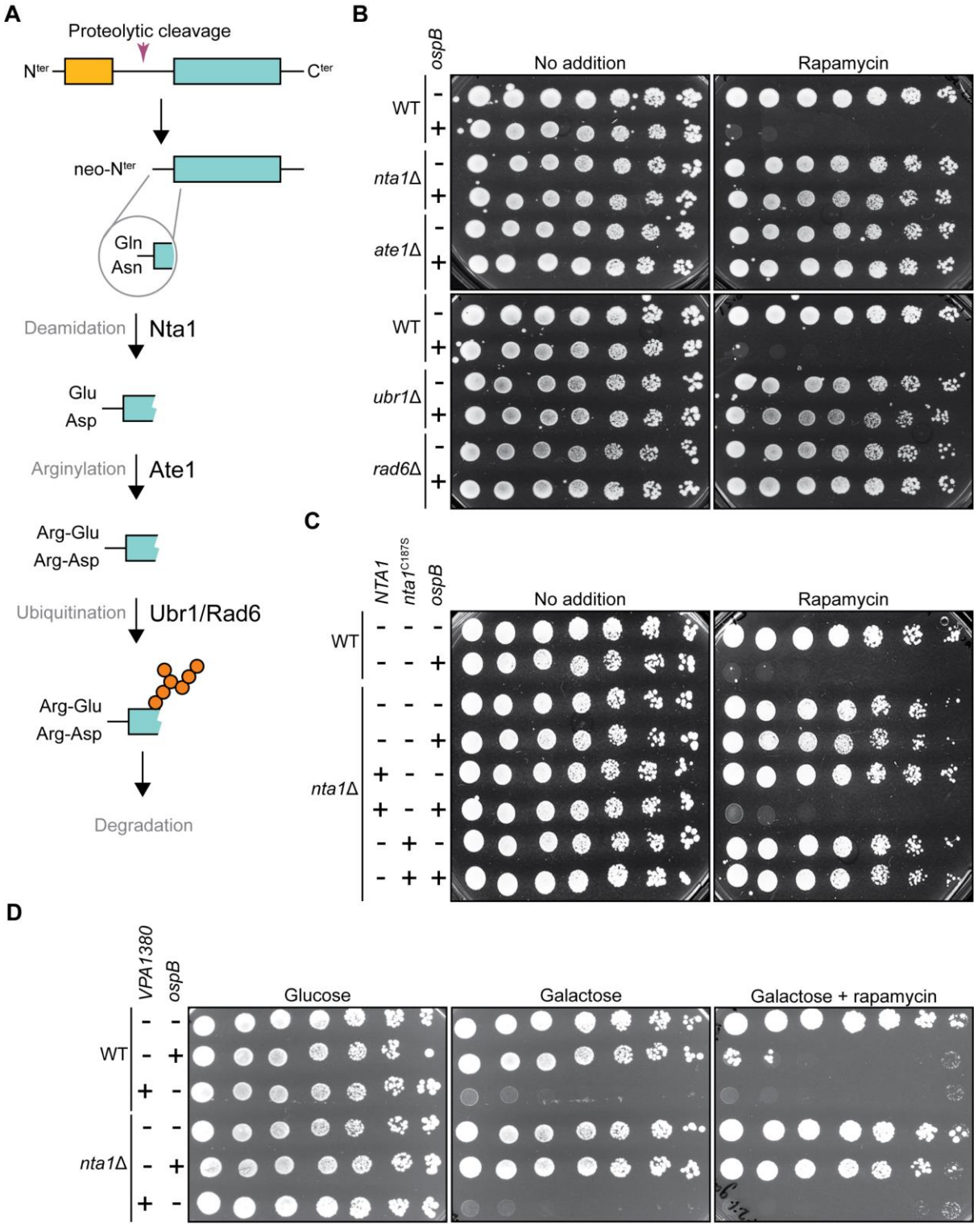

FIGURE 3: The arginine N-degron pathway is required for growth inhibition by OspB.

(A) Schematic of the arginine N-degron pathway.

bioRxiv preprint doi: https://doi.org/10.1101/2021.09.01.458261; this version posted April 1, 2022. The copyright holder for this preprint (which was not certified by peer review) is the author/funder, who has granted bioRxiv a license to display the preprint in perpetuity. It is made available under aCC-BY 4.0 International license.

(B) Growth of yeast strains expressing *ospB* or vector control in the presence or absence of genes encoding components of the arginine N-degron pathway. Serial dilutions were spotted on media with or without rapamycin (n = 3).

(C) Growth of yeast strains expressing *ospB* or vector control in the presence or absence of a functional *NTA1* allele. Serial dilutions were spotted on media with or without rapamycin (n = 3).

(D) Growth of yeast strains expressing *ospB*, *VPA1380*, or vector control in the presence or absence of *NTA1*. Serial dilutions were spotted on media with or without rapamycin, in conditions repressing (glucose) or inducing (galactose) *VPA1380* expression (n = 3).

bioRxiv preprint doi: https://doi.org/10.1101/2021.09.01.458261; this version posted April 1, 2022. The copyright holder for this preprint (which was not certified by peer review) is the author/funder, who has granted bioRxiv a license to display the preprint in perpetuity. It is made available under aCC-BY 4.0 International license.

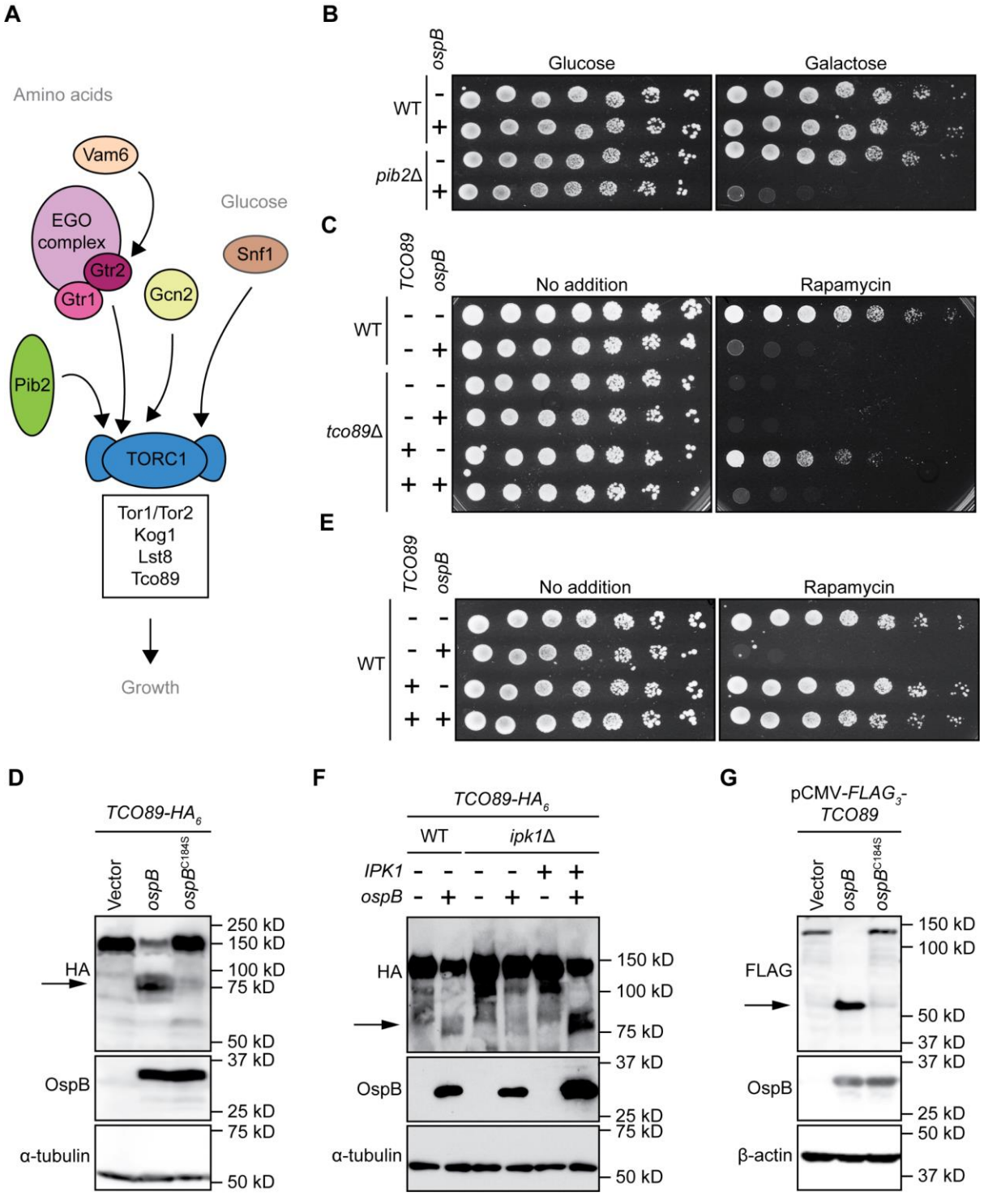

FIGURE 4: The TORC1 subunit Tco89p is cleaved by OspB.

(A) Diagram of the yeast TORC1 signaling network.

(B) Growth of yeast strains expressing *ospB* or vector control in the presence or absence of *PIB2*. Serial dilutions were spotted on media containing glucose (repressing *ospB* expression) or galactose (inducing *ospB* expression) (n = 3).

bioRxiv preprint doi: https://doi.org/10.1101/2021.09.01.458261; this version posted April 1, 2022. The copyright holder for this preprint (which was not certified by peer review) is the author/funder, who has granted bioRxiv a license to display the preprint in perpetuity. It is made available under aCC-BY 4.0 International license.

(C) Growth of yeast strains expressing *ospB* or vector control in the presence or absence of *tco89*. Serial dilutions were spotted on media with or without rapamycin (n = 4).

(D) Western blot assessing cleavage of Tco89p in yeast, in the presence of OspB, OspB(C184S) or vector control. Alpha tubulin is the loading control. The arrow marks the Tco89p C-terminal cleavage product (n = 4).

(E) Growth of wild type yeast expressing *ospB* or vector control, in the presence or absence of *TCO89* expression from a multi-copy plasmid. Serial dilutions were spotted on media with or without rapamycin (n = 3).

(F) Western blot assessing cleavage of Tco89p by OspB in wild type or *ipk1* mutant yeast. Alpha tubulin is the loading control. The arrow marks the Tco89p C-terminal cleavage product (n = 3).

(G) Western blot assessing cleavage of a Tco89p construct expressed in HEK293T cells, in the presence of OspB, OspB(C184S) or vector control. Beta-actin is the loading control. The arrow marks the Tco89p N-terminal cleavage product (n = 3).

bioRxiv preprint doi: https://doi.org/10.1101/2021.09.01.458261; this version posted April 1, 2022. The copyright holder for this preprint (which was not certified by peer review) is the author/funder, who has granted bioRxiv a license to display the preprint in perpetuity. It is made available under aCC-BY 4.0 International license.

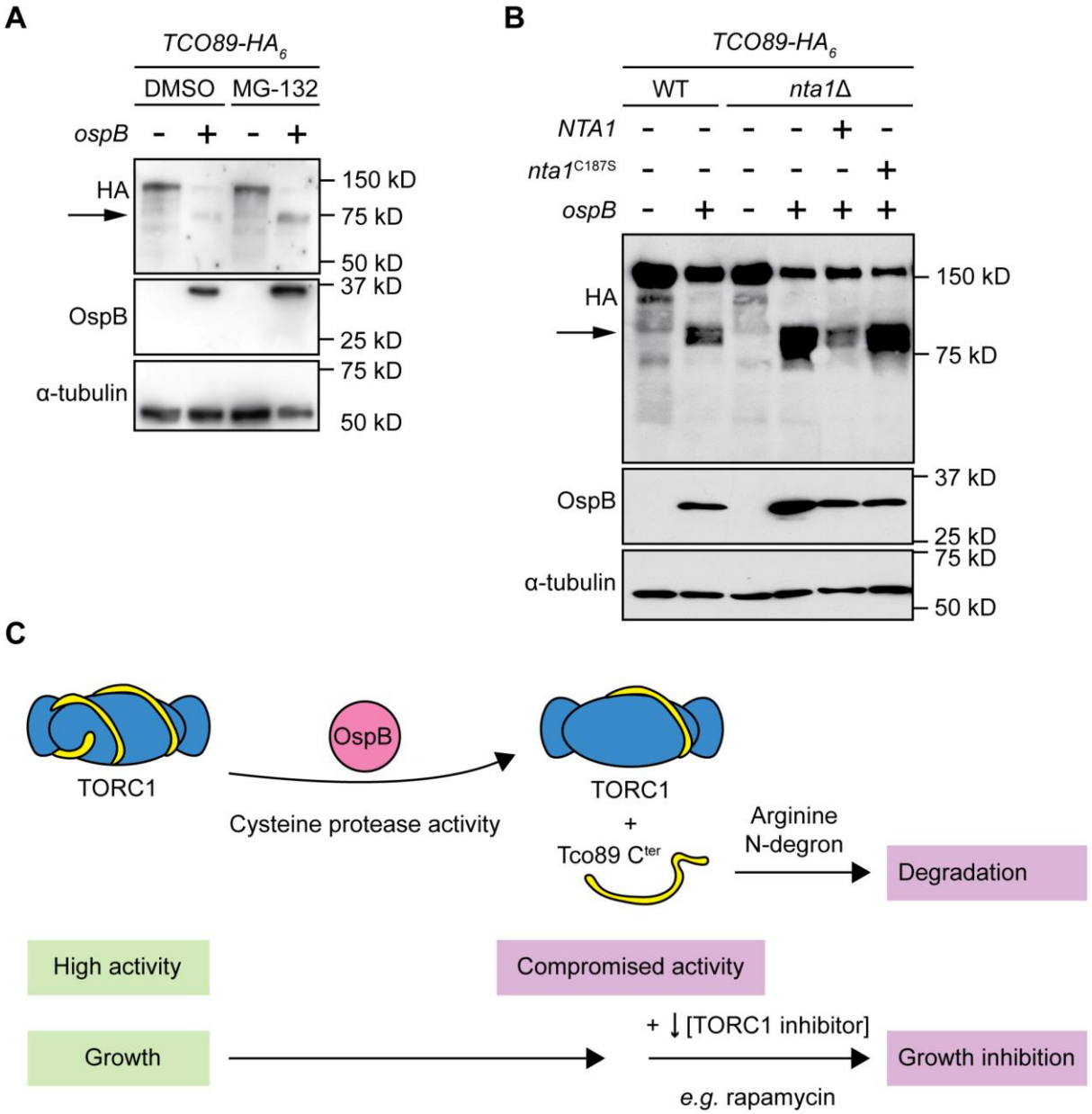

FIGURE 5: Degradation of the Tco89p C-terminal fragment by the arginine N-degron pathway.

(A) Western blot assessing cleavage of Tco89p by OspB in the presence and absence of proteasome inhibitor MG-132. Alpha tubulin acts as a loading control. The arrow marks the Tco89p C-terminal cleavage product (n = 3).

(B) Western blot assessing cleavage of Tco89p by OspB in the presence or absence of a functional *NTA1* allele. Alpha tubulin is the loading control. The arrow marks the Tco89p C-terminal cleavage product (n = 3).

(C) Model of the mechanism of OspB-mediated sensitization of yeast to TORC1 inhibition.